




Article

Recovery of (Z)-13-Docosenamide from Industrial Wastewater and Its Application in the Production of Virgin Polypropylene to Improve the Coefficient of Friction in Film Type Applications

Joaquín Hernández-Fernández ^{1,2,3,*} , Esneyder Puello-Polo ⁴  and Juan López-Martínez ⁵ 

¹ Chemistry Program, Department of Natural and Exact Sciences, San Pablo Campus, University of Cartagena, Cartagena 130015, Colombia

² Chemical Engineering Program, School of Engineering, Universidad Tecnológica de Bolívar, Parque Industrial y Tecnológico Carlos Vélez Pombo, Km 1 Vía Turbaco, Turbaco 130001, Colombia

³ Department of Natural and Exact Science, Universidad de la Costa, Barranquilla 30300, Colombia

⁴ Grupo de Investigación en Oxi/Hidrotratamiento Catalítico y Nuevos Materiales, Programa de Química-Ciencias Básicas, Universidad del Atlántico, Barranquilla 081007, Colombia

⁵ Institute of Materials Technology (ITM), Universitat Politècnica de Valencia (UPV), Plaza Ferrandiz and Carbonell s/n, 03801 Alcoy, Spain

* Correspondence: jhernandezf@unicartagena.edu.co; Tel.: +57-301-5624990

Abstract: Additives play an important role in the production of plastic materials through their application, in which the mechanical, thermal, and physical properties of polymers are improved, making them last longer and be more resistant. During the synthesis of polypropylene resins, the remains of additives that are not absorbed by the resin are removed in the purification stage and end up in the wastewater. In this article, the recovery of (Z)-13-docosenamide from the wastewater from the process, its purification, and its application in the process was carried out. For the extraction of the additive, solid phase extraction (SPE) was used, and to guarantee the purity of (Z)-13-docosenamide, techniques such as high performance liquid chromatography (HPLC), Fourier transform infrared (FTIR), gas chromatography-mass spectrometry (GC/MS), thermogravimetric (TG) coupled with a gas chromatography-mass spectrometry (GC/MS), and differential scanning calorimetry (DSC) were used. The recovered erucamide was added to the PP between 0.05 and 0.3% *w/w*. The effects of the properties of the virgin polypropylene with the recovered additive were also evaluated to determine its effectiveness in improving the properties of the material by measuring the coefficient of friction (CoF) as well as the mechanical properties and wettability through atomic force microscopy (AFM) and the contact angle, respectively. It was discovered that using these techniques, it is possible to recover approximately 95% of the additive present in the water while keeping the material's properties within the desired limits.

Keywords: erucamide; polypropylene; coefficient of friction; recovery; wastewater



Citation: Hernández-Fernández, J.; Puello-Polo, E.; López-Martínez, J. Recovery of (Z)-13-Docosenamide from Industrial Wastewater and Its Application in the Production of Virgin Polypropylene to Improve the Coefficient of Friction in Film Type Applications. *Sustainability* **2023**, *15*, 1247. <https://doi.org/10.3390/su15021247>

Academic Editor: Grigorios L. Kyriakopoulos

Received: 13 September 2022

Revised: 26 December 2022

Accepted: 26 December 2022

Published: 9 January 2023



Copyright: © 2023 by the authors. Licensee MDPI, Basel, Switzerland. This article is an open access article distributed under the terms and conditions of the Creative Commons Attribution (CC BY) license (<https://creativecommons.org/licenses/by/4.0/>).

1. Introduction

The production of plastics has been multiplying more and more in the last 60 years [1], which is due to its versatile and durable inexpensive nature. With the increase in this production, the challenges and opportunities of the industry for the management of the waste generated by the process have also increased [2]. Among the aggressive compounds generated at an industrial level that present great contamination are those present in industrial wastewater, which receives treatment and is later discharged into the aquatic environment, generating contamination by emerging organic pollutants produced by compounds not removed during the treatment [3–6]. Today, there is no regulation of these contaminants and there are no specific methodologies that allow for a chemical characterization of the trace contaminants present in industrial waste generated in petrochemical plants, so it is necessary to develop strategies that allow for the identification of contaminants and their

removal to mitigate their possible impact [7–11]. One of the components that can be found in industrial waste are the additives, which are an essential part of the polymers, since they allow the material to improve its resistance to aging [12–14].

Polymeric additives are materials widely used in various fields such as paint, agriculture, and polymers, to name a few. The various substances used in polymers allow for the improvement in the characteristics of interest at a low cost, and they are classified according to their function [15,16]. These additives can be plasticizers, flame retardants, antioxidants, pigment lubricants, antistatic agents, slip compounds, and heat stabilizers [2,17–20]. Some of the most widely used slip compounds are metal stearates, waxes, and fatty acid amides such as erucamide (13-cis-docosenamide, $C_{22}H_{43}NO$) and primary oleamide, which have been widely used since the late 1960s on an industrial level [21,22]. The main characteristics of erucamide are its stability and transparency, which allows it to be a multifunctional additive. However, it can generate hydroperoxide derivatives through the oxidation of the compound [23–26]. Erucamide is used in the production of polypropylene (PP) as a slip agent, meaning that it reduces the coefficient of friction (CoF) of PP [27]. Erucamide migration, distribution, and nanomechanical properties, along with the effect of the erucamide concentration and ambient temperature on its surface structure, have been widely studied. From these studies, it is clear that the slip-additive surface assembly and the resultant performance depend on the additive deposition method and concentration as well as the substrate surface chemistry. Traditionally, the extraction of erucamide from the matrices of interest has been performed by Soxhlet extraction or reflux, supercritical fluid extraction (SFE), and microwave-assisted extraction (MAE) [28–31]. In the PP production process, there is a stage called deodorization. In this stage, there is a column to which PP, steam, and hot nitrogen are fed. When the steam comes into contact with the PP, it extracts or removes a significant amount of erucamide from the PP. This erucamide migrates to water vapor, which is then condensed and this condensate is stored in a process water collection tank. This water is mixed with the remains of wastewater that are formed in other stages of the process, solid phase extraction (SPE) being the most suitable cleaning technique for this type of sample [32,33]. The SPE has been used to recover additives of different chemical natures and has shown recoveries of more than 80%, especially for highly complex matrices such as industrial wastewater [7].

This research proposes a system for the recovery and purification of erucamide ((Z)-13-docosenamide) present in wastewater from the deodorization of polypropylene for its subsequent application in virgin polypropylene. We used SPE for the removal and purification of erucamide from wastewater. HPLC, GC-MS, TD-GC/MS, FTIR-ATR and DSC were conducted for the identification and quantification of erucamide. The CoF, contact angle, and AFM of the PP films was evaluated to determine the efficiency and efficacy of the added erucamide in this PP.

2. Materials and Methods

2.1. Materials

For this process, analytical-grade reagents were used. HPLC grade methanol and acetonitrile from SDS (Pepyn, France), ammonium clarity, and NaOH (purchased from Merck, Darmstadt, Germany), (Z)-13-docosenamidem, and water, purified with a Milli-Q system (Millipore, Bedford, MA, USA).

2.2. Sampling

Sampling was carried out at a PP production plant. This plant has 4 basic stages for production: (1) The receipt, purification, and storage of propylene; (2) the polymerization process; (3) additivation and pelletization; and (4) deodorization. In Figure 1, the basic scheme of the plant can be observed. In this investigation, we focused on stage 3 and stage 4. In these stages, significant volumes of wastewater are generated, where stage 3 corresponds to additivation and extrusion. In this stage, a package of necessary additives is added so that the PP has the ideal performance in its final applications. In the extrusion process,

the PP resin is mixed with the additive package, then the material passes to different heating zones between 190 and 230 °C. In this process, the mixture of PP and additives melt and a homogeneous melt is obtained. This melt is then cooled and passes to the cutting areas, where the effect of some blades cuts the melt into small spheres. In this cutting process, significant amounts of water are added to make the cut cold and avoid the high deterioration of the blades. In this investigation, we wanted to evaluate the quantities of erucamide that migrated into the water. If the amount of erucamide is of interest, then the erucamide should be recovered. For the PP manufacturing process, it is necessary to use a desorber to remove volatile chemical residues that can cause unpleasant odors. To ensure the efficiency of this desorber, steam and N₂ are injected into the desorber column for approximately 4 h. Experimentally, it has been shown that this time of 4 h is the most optimal. Table 1 shows the sampling plan to determine the points of interest to evaluate the recovery of erucamide.

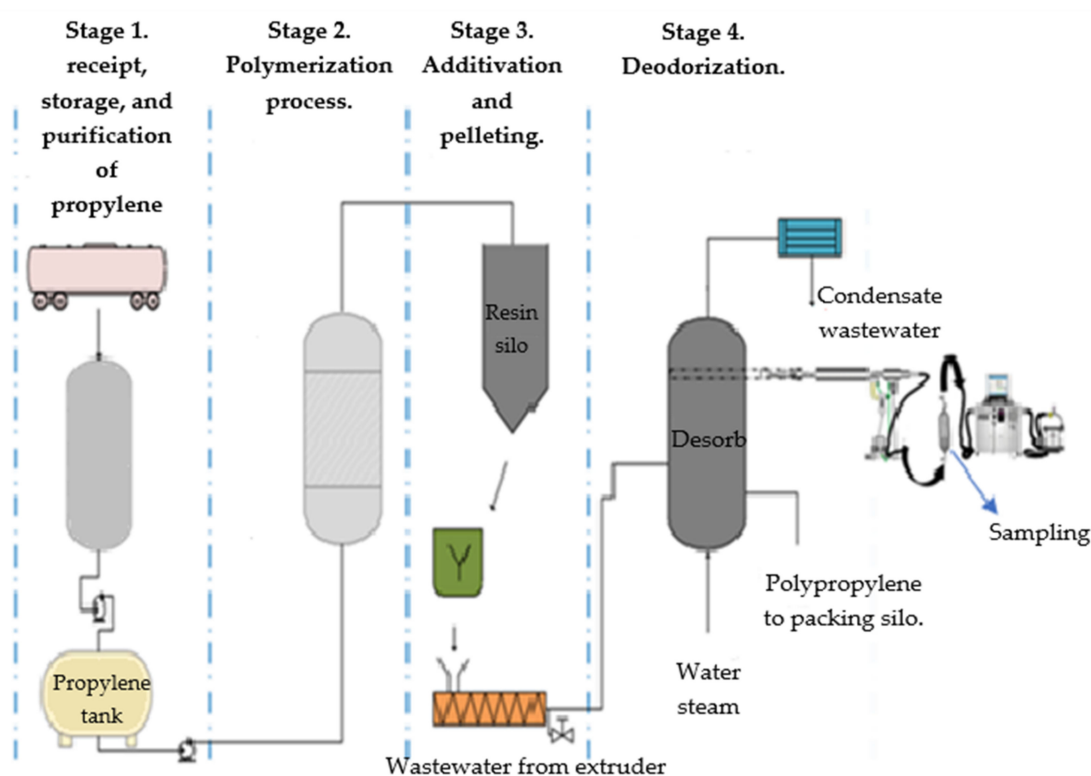


Figure 1. Summary of the five principal stages of PP production.

Table 1. Sampling plan and point of interest.

Sample Point	Zone	Sample	Sample Rate	Objective
Stage 3	Extruder outlet	Wastewater	4 h/30 days	Identification, quantification, and recovery of erucamide
Stage 4	Top deodorant	Gases	4 h/30 days	
Stage 4	Bottom desorber	Wastewater	4 h/30 days	

A prototype that permitted modeling of the deodorization process was created for this method [7,34]. Since the liquid generated during this process may contain traces of additives that are generally treated as wastewater from this stage of the process, 100 mL of the desorber condensate was taken. A sample was taken every 30 min for a total period of four hours, totaling 10 samples. From this sampling, a representative sample was taken, which was stored in an amber glass at a temperature of 4 °C.

2.3. Preparation of Industrial Wastewater Samples

To avoid possible separation of the compounds present in the sample, it was homogenized and tempered at 25 °C to avoid activation of the additive and enzymatic degradation occurring. Subsequently, it was filtered using a Teflon filter and the resulting sample was diluted with 100 mL of acetonitrile in a volumetric balloon until reaching a volume of 500 mg L⁻¹, of which 2.5 mL was diluted again with acetonitrile to reach a volume of 50 mL.

2.4. Gas Sample Taking

The sampling of the gases in the upper part of the desorber was a capacity of 1000 mL including a relief valve. The valve's relief was adjusted for pressure between 300 and 400 psi. The cylinders were equipped with a maximum level indicator tube (deep tube) that permitted the release of 20% of the capacity of the container. The desorber had a sampling point located 1 m from the high point of the column. This point had a nipple, and a flute-shaped steel tube with a longitude equal to the diameter of the column. This flute had 20 equidistant orifices that permitted the sampling of more than 95% of the diameter of the column. The end of the flute had two exits, one of which was connected to a constant pressure vacuum pump, and the other, with a metallic cylinder covered with sulfinert. This system permitted us to take an isokinetic sample in such a way that each of the 20 orifices had the same pressure, and therefore, each one took in the same amount of the sample. The 20 orifices permitted the entry of more than 95% of the laminar flow of gases from the column, guaranteeing a representative isokinetic sample. In each orifice, the gases were mixed in the interior of the flute, and were later collected in the interior of the steel cylinder covered with sulfinert. The time of desorption of each grade of PP in the desorber was 4 h, and the samples were taken in triplicate

2.5. Additive Recuperation

2.5.1. Extraction of Solid Phases

After the pretreatment, a solid phase extraction (SPE) was carried out to concentrate and purify the sample, where the liquid that came out was collected and the solvent was evaporated by means of a nitrogen current (N₂), thus leaving the solid compounds of the crystallized mixture. For this stage, a 12-port solid phase extraction equipment (Phenomenex) was used [35].

Methodology for Quantifying in Liquid Waste

The analyses were performed using Agilent 1100 HPLC equipment with the following modules: degassing unit (G1322A), quaternary pump (G1311A), auto sampler system (G1313A), column carrier (G1316A), and a DAD detector (G1315B) with the Chemstation data acquisition system. A Lichrosorb RP-18 column (4.6 mm × 200 mm × 5 mm), 5 and 10 mL syringes, and a precision balance (Mettler-Toledo, Barcelona, España) were also utilized.

Treatment of Samples Based on SPE

1. Pretreatment

The work sample was homogenized and tempered at 25 °C, and then filtered in a PTFE Teflon filter of 0.22 m to facilitate the subsequent sample preparation and reduce the microbial activity.

2. Preconcentration and Cleaning

At this stage, the conditioning of Strata X-33 cartridges (6 mL, 500 mg) was performed with 5 mL of MeOH followed by 5 mL of distilled water. Subsequently, 15 mL of the sample was uploaded at a rate of 1 mL min⁻¹. Once the entire sample was percolated, the cartridges were washed with 3 mL of MeOH:H₂O at 80:20. Elution of the compounds retained in the solid phase was performed with 10 mL of ACN. The eluate was evaporated

until dry with a stream of nitrogen at 5 psi. The final extract was reconstituted with ACN to a final volume of 1 mL, obtaining a pre-concentration of 10:1.

2.5.2. Chromatographic Analysis (HPLC-DAD)

By means of a chromatographic analysis (HPLC), it was possible to determine the analyte of interest and subsequently proceed to efficiently recover (Z)-13-docosenamide. At this stage, an Agilent 1100 HPLC system with modules is required [36]. The separation was performed in a Lichrosorb column RP 18 (4.6 m × 200 mm × 5 m) from Phenomenex with a programmed gradient combination of solvents A (ACN) and B (H₂O) under the following conditions: 84% A and 16% B (1 min, 1.5 mL min⁻¹); A 92% and 8% B (2 min, 2.0 mL min⁻¹); 96% A and 4% B (3.5 min, 3.5 mL min⁻¹); 100% A and 0% B (8 min, 3.5 mL min⁻¹). The column temperature was 50 °C, with an injection volume of 20 mL.

2.5.3. Fourier Transform Infrared Spectroscopy (FTIR)

Fourier transform infrared spectroscopy (FTIR) was used to follow the structural changes of the polymeric matrix due to induced thermal degradation after exposure to a high temperature of 400 °C. FTIR analysis was performed using a Nicolet 6700 infrared spectrometer (Thermo Scientific, Waltham, MA, USA). Each measurement was performed between 4000 and 600 cm⁻¹ with a resolution of 2 cm⁻¹ in the reflection mode.

2.5.4. Differential Scanning Calorimeter (DSC)

The differential scanning calorimeter (DSC) used was a Perkin Elmer DSC Q2000 V24.11. The study was performed using samples weighing between 5 mg. These were then heated from 40 to 350 °C at a rate of 20 °C min⁻¹ in a nitrogen atmosphere [37,38].

2.5.5. Gas Chromatograph-Mass Spectrometry (GC-MS)

Quantification was performed using a gas chromatograph (Agilent 7890B, Santa Clara, CA, USA) with a front injector (250 °C, 7.88 psi, 33 mL min⁻¹) and a back injector (250 °C, 11.73 psi, 13 mL min⁻¹). The oven was started at 40 °C × 3 min, increased to 60 °C at 10 °C min⁻¹ × 4 min, and increased again to 170 °C at 35 °C min⁻¹. The MS (Agilent 5977A) was fitted with a 170 mm × 0.11 mm fused-silica restrictor (Agilent G3185-60362) to achieve a fixed flow rate of 1.4 mL min⁻¹ He. The system worked in selected ion monitoring (SIM) mode.

2.5.6. TD-GC/MS Chromatographic Conditions

Thermogravimetric (TG) (NETZSCH STA449 F3) coupled with gas chromatography-mass spectrometry (GC/MS) was used. About 15 mg of the sample was pyrolyzed/combusted between 40 °C and 800 °C at 10 °C/min. Helium with a flow rate of 20 mL/min was used as the carrier gas to create an inert atmosphere in the pyrolysis process, while the mixtures of 16 mL/min helium and 4 mL/min oxygen were used as the oxidative atmospheres for the incineration experiment.

2.6. (Z)-13-Docosenamide Add-On Recovered with the PP Matrix

Following the recovery of (Z)-13-docosenamide, this was followed by mixing it with the PP (virgin-without additives) with a standard Prodex Henschel 115JSS mixer at 800 rpm for a period of 15 min at room temperature [39]. The mixture was then passed to an extruder. The extruder worked with five heating zones, which were 190, 195, 200, 220, and 230. After melting during transportation, the product was passed through a polymeric matrix and solidified by immersion in water. The resultant solid was then compacted to provide small irregularly shaped granules. Table 2 shows the samples prepared with the necessary amounts of erucamide.

Table 2. Preparation of the mixtures of virgin PP and erucamide recovered.

Samples	Recovered Erucamide Added (mg)	Virgin PP Resin Added (Kg)
PP1	0	1
PP2	500	1
PP3	1000	1
PP4	1500	1
PP5	2000	1
PP6	2500	1
PP7	3000	1

2.6.1. Fourier Transform Infrared (FTIR)

FTIR was used to measure the structural changes of the polymeric matrix, since, when exposed to high temperatures (400 °C), a thermal degradation of the matrix occurs. A Nicolet 6700 FTIR (Thermo Scientific) was used [40].

2.6.2. Friction Coefficient (CoF)

A slip and friction tester (Model 32-07; Testing Machines, Inc., New Castle, DE, USA) was used to measure the CoF (ASTM D1894). The coefficient of friction (CoF) was calculated by dividing the kinetic force (fk), which is necessary to move one surface over another [27,41].

2.6.3. Contact Angle Measurement of PP–Erucamide Films

A Drop Shape Analyzer–DSA100 (KRÜSS) unit operated with the KRÜSS ADVANCE 1.9.0.8 software was used, using 10 mL of MilliQ water (resistivity of 18.2 MX.cm at 25 °C) as a liquid probe. The drop image was recorded for 60 s at 2 s intervals. Measurements were made at a temperature of 20 ± 0.5 °C.

2.6.4. Atomic Force Microscopy (AFM) Measurement of PP–Erucamide Films

The FMA was used to determine the modulus of elasticity of the surface of films from PP1 to PP7. For this purpose, an atomic force microscope (Veeco Nanoscope) working in maximum force mode was used. The force curves were recorded and fitted to mathematical models to obtain the elastic maps of the square areas of 10×10 µm.

3. Results and Discussion

3.1. Recovery of (Z)-13-Docosenamide

For the correct identification and quantification of (Z)-13-docosenamide, separation by solid phase extraction was started, which is an easy method with rapid execution and very precise results. Once the erucamide had been separated from the wastewater, it was quantified and optimized by HPLC. The measurements of the erucamide concentrations at the top of the desorber, bottom of the desorber, and exit from the extruder are shown in Table 3. These results indicate that the erucamide concentrations in the gas phase were not significant, and that these concentrations ranged from 0.1 to 11 ppm. The recovery system was applied to this sample and the recoveries were 92%. Although the recovery rates are important, the amount recovered is not of interest compared to the investment in materials, reagents, and the researchers' time. The sampling period carried out at the bottom of the desorber allowed for the identification of erucamide concentrations in the range of 300 to 600 ppm. At this point, the recoveries were 95%. At the exit of the extruder, the concentrations of erucamide ranged between 700 and 900 ppm. This highlights that the volume of water generated at the top of the desorber and at the exit of the extruder is very significant, which is why the recovery of erucamide was implemented for one year. This recovered and purified product was characterized with different instrumental techniques

and later applied to virgin PP resins to evaluate its performance. The results showed that the recovery percentages of (Z)-13-docosenamide were above 95%. Therefore, the ability to separate this compound is essential, since it allows the degree of contamination in wastewater to be significantly reduced, which favors environmental regulations and the protection of public health.

Table 3. Preparation of mixtures of the virgin PP and erucamide recovered.

Sampling Point	Sample Status	Erucamide Concentration Range (ppm)	Preconcentration Factor	Recovery (% w/w)
Top desorber	Gases	0.1–11	100	92
Bottom desorber	Wastewater	300–600	100	95
Extruder outlet	Wastewater	700–900	100	95

3.2. Identification and Verification of the Purity of (Z)-13-Docosenamide

3.2.1. Fourier Transform Infrared (FTIR)

The characteristic functional groups of the analysis by means of the FTIR were identified and it was verified whether there was the presence of compounds other than the one of interest that would affect the quality of the recovered additive. Figure 2 shows the FTIR of the recovered additive, where the functional groups NH₂ (stress vibration at 3312 cm⁻¹ characteristic of primary and secondary amides), C-H= (stress vibration at 3100 cm⁻¹ characteristic of an average intensity of carbon–hydrogen bonds of alkenes), CH (stress vibration at 2841 cm⁻¹ typical of linear aliphatic alkanes chains, corresponding to the hydrophobic chain of erucamide), C=O (1695 cm⁻¹, refers to the carbonyl group present in the amido group of erucamide, which is known as the hydrophilic head), CH₂ (bending vibration at 1465 cm⁻¹), and C–N (bending vibration at 1350 cm⁻¹), characteristic of (Z)-13-docosenamide, are evident. The information gleaned from this analysis was compared to records in the literature to see whether they corresponded to erucamide, indicating that the compound obtained was of acceptable purity and did not contain compounds that could impair its application performance [42,43].

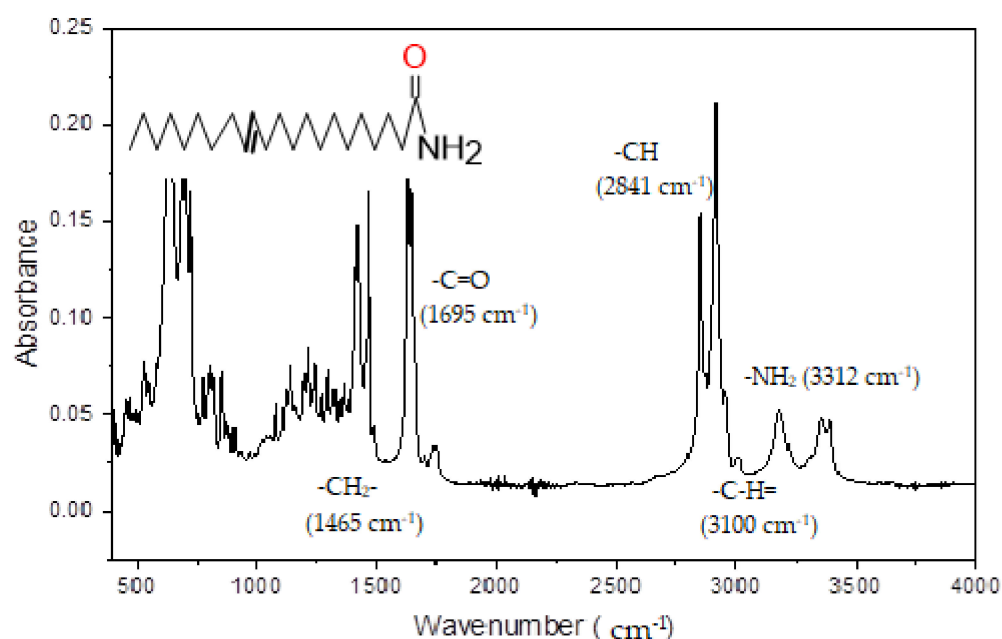


Figure 2. IR spectrum of the recovered erucamide.

3.2.2. Identification and Characterization of Erucamide for GC-MS

The recovered erucamide was analyzed by GC-MS to determine its purity by evaluating its mass spectrum. Figure 3 shows the mass spectrum. A very characteristic spectrum of linear hydrocarbons was observed. In Figure 4, we propose a fragmentation mechanism that can help us to elucidate the structure by proposing specific fragmentation patterns. Figure 3 shows that the peaks with the most stable M/Z ratios were 126, 112, 72, 69, 67, 59, 57, 55, 43, and 41. In the spectrum, it was observed that many peaks were the result of the loss of small molecules due to the common decomposition of ions with an even number of electrons. Thus, a peak of good abundance can appear two more units below an ion with an abundant number of electrons due to the loss of a hydrogen molecule, and cause another homologous series of ions with an even number of electrons whose structural significance could be misleading. Due to the above, in Figure 4, fragmentation of hydrocarbons could be observed that corresponded to M/Z 41, 55, 67, and 69. The fragmented ions with M/Z 43, 57, 59, 72, 112, and 126 corresponded to the chain fragmentation near the amide group and H-H bond breaks.

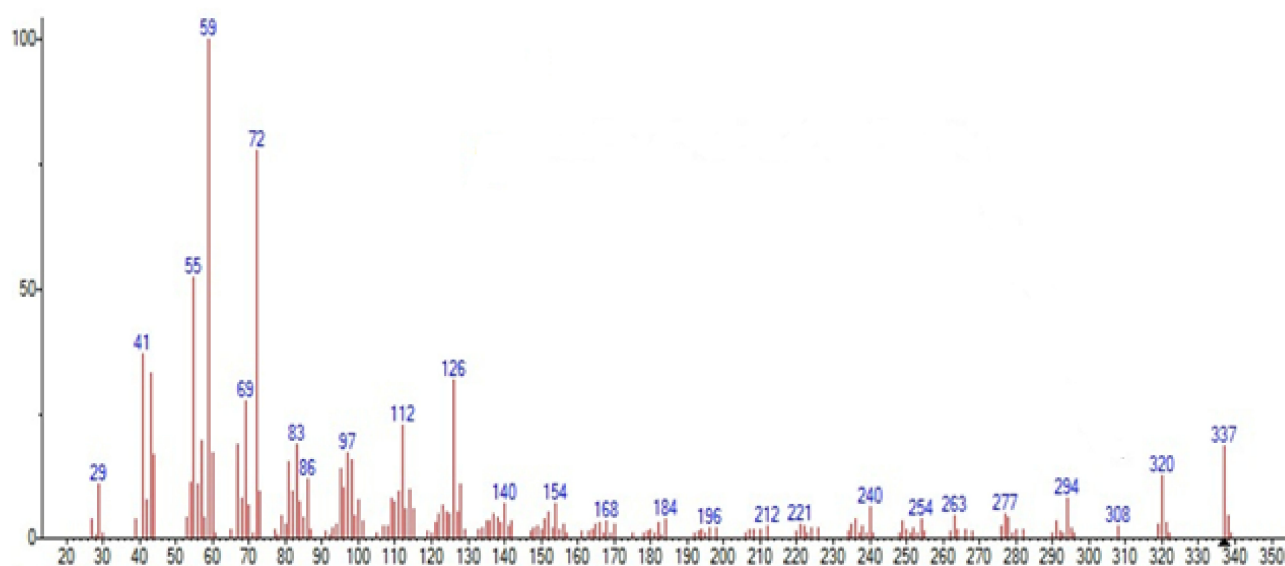


Figure 3. MS spectrum of the recovered erucamide.

3.2.3. Identification and Characterization of Erucamide Degradants by High-Resolution Mass Spectrometry

Table 4 reports the retention time (Tr) of the identified molecules, the names of these compounds, the molecular weight, the chemical formula, and the most characteristic fragments. The erucamide analysis was conducted separately on positive and negative modes of ESI without mobile phase flow splitting. In the present analysis, molecules were identified that were associated with the presence of erucamide impurities and other results of the degradation of the erucamide molecule. The result of the chromatography allowed us to find information such as the retention times, theoretical and observed mass, the main erucamide MS fragments, and their degradation products. With this information, we propose the suggested molecular formula based on the exact mass and isotopic fidelity. All of the information described above is tabulated in Table 4. In Table 4, we present the oxidized derivatives of erucamide. These derivatives contain the same number of carbon atoms of erucamide. The formation of the derivatives of hydrogen peroxides that are listed in Table 4 occurs through the extraction of hydrogen from peroxy radicals. Table 4 also reports the molecules with the presence of double bonds, which makes unsaturated fatty acids more prone to hydrogen extraction due to less dissociation energy compared to the saturated aliphatic chains. It is important to note that hydroperoxides are very unstable, which causes them to decompose further to form alkoxy radicals, which in turn undergo

β -cleavage at both sides of the alkoxy carbon to produce aldehyde, ketone, and carboxylic acid species.

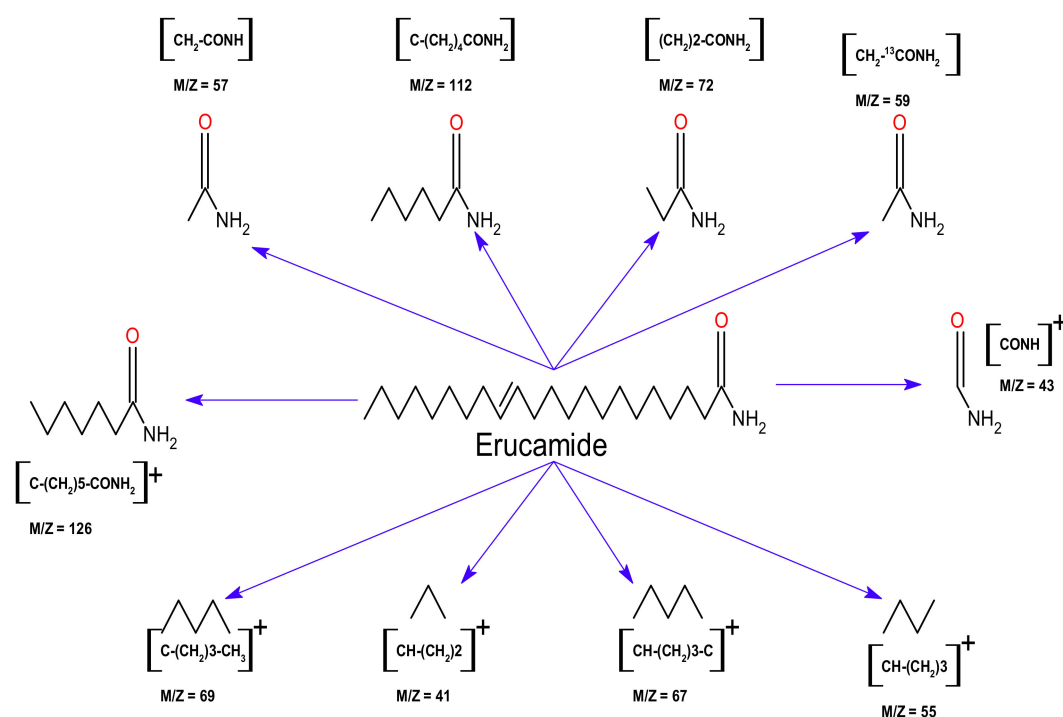


Figure 4. Recovered erucamide fragmentation mechanism.

Table 4. Mass of the recovered erucamide oxidation products.

Tr (Min)	Compound	Mass	Formula	Fragments
3.06	12-amino-12-oxo-dodecanoic acid	228.16	C ₁₂ H ₂₃ NO ₃	211.13, 210.15, 184.17, 167.14
4.34	14-amino-14-oxotetradecanoic acid	256.2	C ₁₄ H ₂₇ NO ₃	239.16, 212.2, 238.18 195.17
6.58	14-oxotetradecanamide	242.2	C ₁₄ H ₂₇ NO ₂	225.18, 207.17, 197.2
7.26	15-oxopentadec-13-enamide	254.21	C ₁₅ H ₂₇ NO ₂	239.2, 237.18, 219.17, 201.16
7.85	Undecanamide	186.18	C ₁₁ H ₂₃ NO	169.16, 158.15, 151.08
8.8	Erucamide keto-epoxide	368.3	C ₂₂ H ₄₁ NO ₃	351.29, 352.32, 333.28, 315.27
10.78	Erucamide with ketone	352.3	C ₂₂ H ₄₁ NO ₂	335.29, 317.28, 307.29, 299.27
11.3	Erucamide with one -OH	354.3	C ₂₂ H ₄₃ NO ₂	337.31, 336.33, 319.29, 309.31, 301.29
12	Cis-11-eicosenamide	310.3	C ₂₀ H ₃₉ NO	293.28, 275.27
13	Erucamide (13-cis-Docosenamide)	338.3	C ₂₂ H ₄₃ NO	321.32, 303.31

The reaction with oxygen leads to the formation of aldehydes such as nonanal, 13-oxotridecanamide, 2-decenal, and dodecanamide. These are formed by the β cleavage of the alkoxy radicals formed at the C14 position of erucamide. Aldehydes, which are the main oxidative products, can also form respective fatty acids due to over oxidation, for example: 13-oxotridecanamide undergoes autoxidation to form 13-amino-13-oxotridecanoic acid. Similar mechanisms can be postulated for the C14, C12, and C15 hydroperoxides of erucamide. The oxidation of erucamide at C14 results in 14-oxotetradec-12-enamide transforming into 14-amino-14-oxo-tetradecanoic acid, respectively. The oxidation at C12 of erucamide yields 12-oxododecanamide (overoxidized to 12-amino-12-oxododecanoic acid) and undecanamide. Alternatively, oxidation at C15 produces 15-oxopentadec-13-enamide and 14-oxotetradecanamide. As a result of over oxidation, 15-oxopentadec-13-enamide

and 14-oxotetradecanamide form 15-amino-15-oxo-pentadec-2-enoic acid and 14-amino-14-oxotetradecanoic acid, respectively. The decomposition products of this process are aldehydes, ketones, carboxylic acids, alcohols, epoxides, and hydrocarbons such as those reported in Table 4.

3.2.4. Differential Scanning Spectroscopy (DSC)

The recovered (Z)-13-docosenamide sample was subjected to a fixed thermal cycle using DSC to study the behavior of the additive by identifying its melting point, as shown in Figure 5, where the behavior of the additive could be observed in a range of temperatures from 50 to 350 °C, obtained at a nominal heating rate of 20 °C/min to detect small heat change transitions. The maximum melting point of the additive was identified at 83.36 °C, a temperature that did not differ from the records of pure erucamide, which has a melting point of 83.5 °C. This allows us to state that the recovered clear changes had a high purity. The melting peak of (Z)-13-docosenamide, on the other hand, was calculated to start at roughly 70.0 °C, which shows that some fractions of (Z)-13-docosenamide started to melt at temperatures significantly lower than its melting point. Erucamide may soften locally during this process, which might aid in the development of a shell/core microstructure [44].

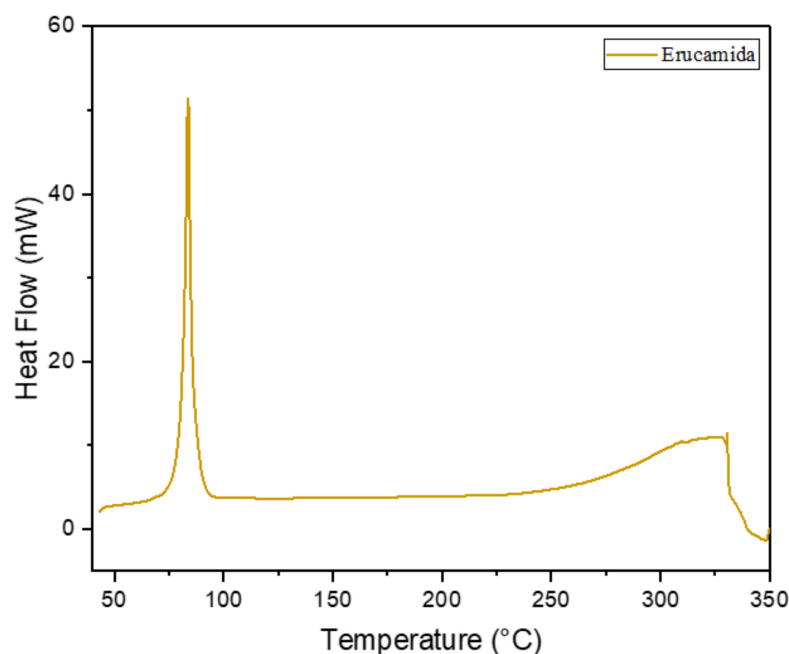


Figure 5. DSC of the recovered (Z)-13-docosenamide.

3.3. Addition of Recovered (Z)-13-Docosenamide Quench to the PP Matrix

The additive was added to the process following the procedure established for the virgin PP resin and was studied as to whether it was absorbed and the effects it had on its properties. For this purpose, we prepared samples of virgin PP and erucamide recovered from wastewater. We prepared seven samples identified as PP1, PP2, PP3, PP4, PP5, PP6, and PP7, as shown in Table 2. Concentrations of erucamide between 0 and 3000 mg were added to each of these samples.

3.3.1. FTIR of the PP Resins with the Recovered Additive

Once the (Z)-13-docosenamide was applied to the PP matrix, the analysis was carried out by means of FTIR, which was used to monitor the quantity and/or concentration of the additive present near the surface of the film [45]. For this technique, it is imperative that the path of the infrared beam remains constant. This is in order to efficiently compare the concentrations of the primary amide throughout the thickness of the film in different spatial locations. In Figure 6, it is possible to observe the spectra related to the concentration of

erucamide in PP, which followed the same pattern but with increased bands, which was due to stretching of the carbonyl group (C=O) and bending of the primary amide (NH₂). As the concentration of erucamide from PP1 to PP7 increased, it was observed that the spectral behavior underwent changes and these changes were more notable for the zone of the carbonyl group and amide. Figure 2 shows that the previously mentioned bands grew or increased their values in areas under the curve as the concentration of erucamide increased.

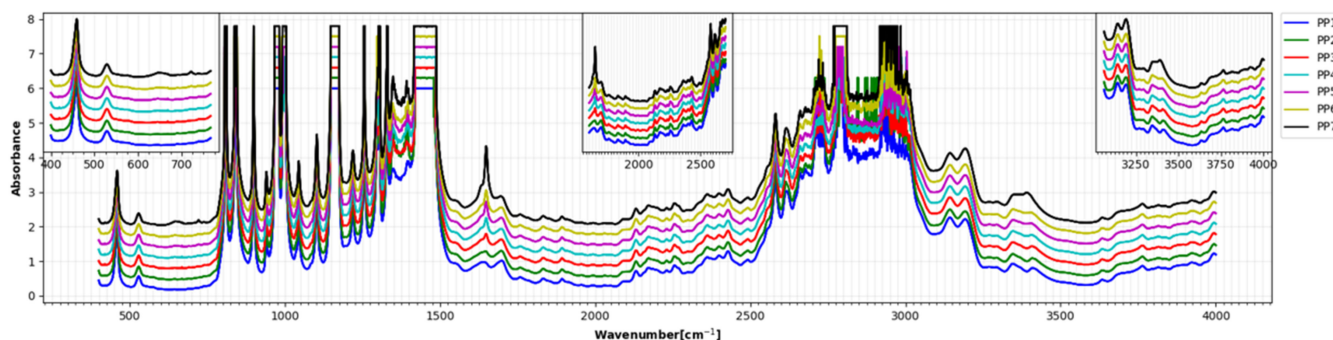


Figure 6. IR spectrum of the PP resins with different concentrations of the recovered erucamide.

3.3.2. PP Resin CoF

The primary function of a slip agent is to reduce the coefficient of friction, which is accomplished by reducing the adhesion of a plastic material to itself, thus minimizing stickiness. See Figure 7. For this function to be fulfilled, it is necessary for the slip agent to have limited compatibility with the polymer so that it can exude toward the surface and provide the plastic with an invisible coating. To determine to what extent the slip agent fulfills its primary function, the CoF was evaluated according to ASTM D1894. A range of 0.8–1.0 is considered no slip; 0.4–0.7 is considered low slip; 0.2–0.4 is considered medium slip; and 0–0.2 is considered high slip. The aim of this study was to correlate the concentration of (Z)-13-docosenamide with COF, as shown below in Figure 8.

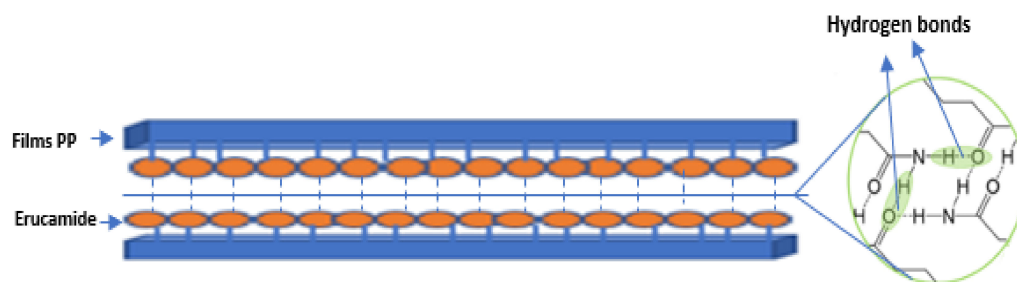


Figure 7. Representation of the migration of erucamide molecules and the formation of hydrogen bonds.

The CoF graph in Figure 8 indicates that as the concentration of recovered (Z)-13-docosenamide increased, the CoF reduction depends on the concentration of (Z)-13-docosenamide, its process diffusion, and film thickness. Initially, the COF was observed at 1, and as time passed, it tended to stabilize at approximately 0.22 [27]. Therefore, it remained within the recommended levels to facilitate the sliding of the film on the surface. According to the formulations above-mentioned, it was reported that at CoF levels between 0.2 and 0.4, therefore, according to what could be observed in the graph, the results were at a medium slip level. It is also possible to analyze that throughout the process, no significant changes were observed in the coefficient of friction values. Therefore, there was no excessive migration of (Z)-13-docosenamide toward the surface of the PP film. Figure 7 is a representation of the migration of erucamide to the surface of the film. In this way, the hydrophobic chains remain immersed in the PP matrix while the amide groups migrate

to the surface. As shown in Figure 7, when these amide groups meet other amide groups, they form hydrogen oxides that allow the films to not remain 100% adhered.

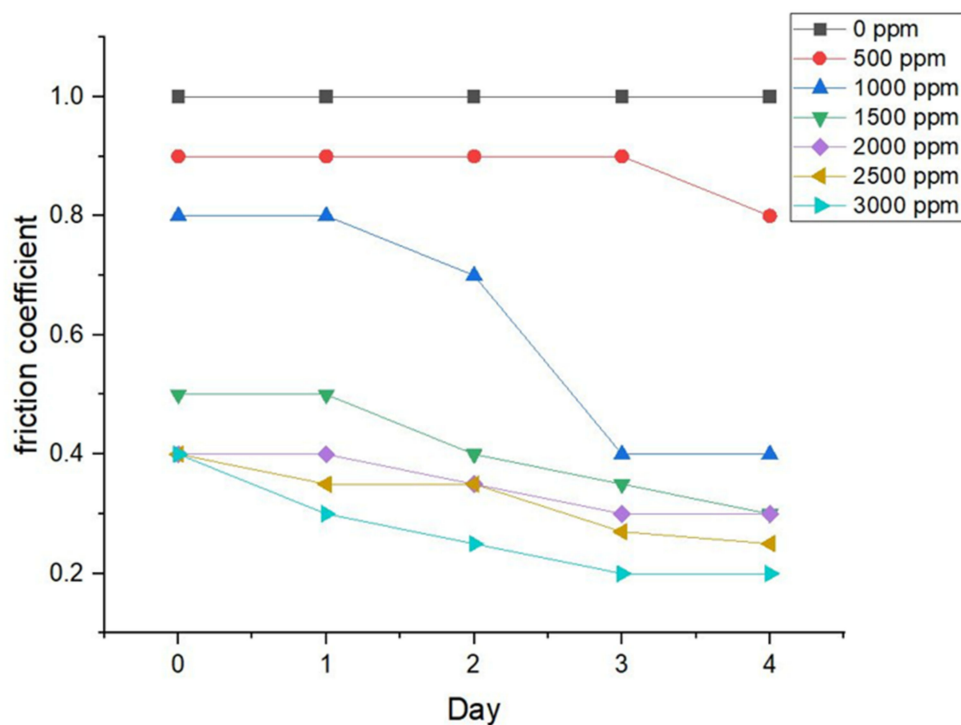


Figure 8. CoF of the PP samples with varying concentrations of the recovered additive.

3.3.3. Contact Angle Measurement of PP–Erucamide Films

The wettability study further confirmed the general molecular orientation of erucamide (i.e., the hydrophobic tails of the CH₃–CH₂-chains pointing outward in the outermost layer of the PP1 to PP7 films). Contact angle measurements revealed an increase in the surface hydrophobicity with an increasing concentration of erucamide in the spin coating solution with the contact angle of water increasing from $85.2 \pm 1.7^\circ$ for PP1 to $90.6 \pm 1.3^\circ$, $93.4 \pm 0.8^\circ$, $95.1 \pm 1.5^\circ$, $95.9 \pm 1.2^\circ$, $96.2 \pm 1.4^\circ$, and $97.4 \pm 1.3^\circ$ for PP2, PP3, PP4, PP5, PP6, and PP7, respectively.

As seen in Table 5, the contact angles from PP1 to PP7 were ≥ 85 , probably due to low surface coverage, as confirmed by the AFM image, which showed isolated aggregates. Thus, an increase in the concentration of erucamide showed an increase in the contact angle and greater hydrophobicity.

Table 5. Contact angles of the virgin PP films and PP films with different concentrations of recovered erucamide.

Samples	Water Contact Angle ($^\circ\theta$)
PP1	85.2 ± 1.7
PP2	90.6 ± 1.3
PP3	93.4 ± 0.8
PP4	95.1 ± 1.5
PP5	95.9 ± 1.2
PP6	96.2 ± 1.4
PP7	97.4 ± 1.3

3.3.4. Atomic Force Microscopy (AFM) Measurement of PP–Erucamide Films

Quantitative nanomechanical AFM mapping (QNM) allowed us to correlate the nanomechanics properties (i.e., adhesive response) and topographical aspects of the chemical structure of the erucamide molecule. In these tests, it was possible to show that the aggregates identified and observed in the images in Figure 9 exhibited a lower adhesive response toward the AFM silicone tip compared to the innermost part of the PP film. As shown in Figure 7, the molecular orientation of the exposed erucamide hydrocarbon tails was outside. Furthermore, the adhesive response differed between that observed within a single aggregate, with the central section and the interior of the aggregates. The measurements showed a variation in the adhesive response as a function of the erucamide concentration. During the measurements carried out by AFM, some important changes were observed during the scan of the tip. The latter may be related to what was observed in Figure 7. This is as if the tip first came into contact with the amide groups that were on the surface, and then with the hydrocarbon tail. In general, the presence of erucamide led to a decreased adhesive response, demonstrating its effectiveness to adjust the nanomechanical properties of the surface, making it less “sticky”. It can be seen that this stickiness decreased with increasing erucamide concentration. The highest value of the elastic modulus was obtained for PP1, which corresponded to pure PP ($E = 2.26$ GPa). However, erucamide addition decreased this value, achieving lower modules in PP7 ($E = 1.67$ GPa), PP6 ($E = 1.82$ GPa), PP5 ($E = 1.87$ GPa), PP4 ($E = 1.95$ GPa), PP3 ($E = 2.01$ GPa), and PP2 ($E = 2.09$ GPa), probably due to the fact that the erucamide molecule can produce some kind of plasticizing effect.

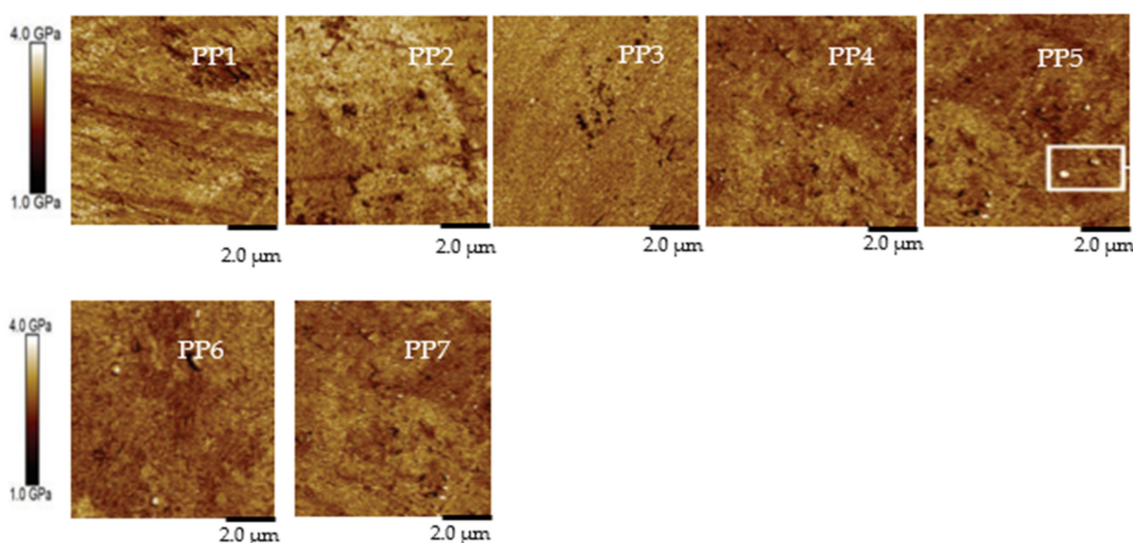


Figure 9. AFM images of the PP resins with different concentrations of the recovered erucamide.

4. Conclusions

In this work, the potential of industrial waste as a source of raw materials used in processes was evidenced through the characterization and extration of the components of interest, preventing them from being discharged into water, thereby reducing the environmental impact and reducing the purchase of used inputs during the process.

The SPE method shows great potential for the quantification of (Z)-13-docosenamide in effluents since the extracted sample was successfully recovered, obtaining a recovery percentage above 95%. The foregoing makes this method a fundamental tool when it comes to optimizing the production processes and making them environmentally friendlier. The FTIR and DSC methods confirmed the presence of (Z)-13-docosenamide in the sample, since it presented the characteristic peaks of this additive and, on the other hand, the melting point varied minimally, approximately 0.1 °C. In this way, we guarantee that our recovered additive is pure and not degraded or oxidized. In the GC-MS, fragmentation patterns

typical of erucamide could be observed, which guarantees complete characterization. The analysis by TG-GC/MS shows the fragmentation patterns of the oxidized chemical species of erucamide.

The results presented show the decreasing trend in CoF as a function of concentration until its stabilization was generated by the slippery additive in the PP films. The relationship presented here to analyze this behavior was through the ASTM D1894 standard. The results indicate that the concentrations of (Z)-13-docosenamide showed a moderate migration toward the PP surface, which may be due to the degree of oxidation of the film. The measurements showed a variation in the adhesive response as a function of the erucamide concentration. During the measurements carried out by AFM, some important changes were observed during the scan of the tip. In general, the presence of erucamide led to a decreased adhesive response, demonstrating its effectiveness for adjusting the nanomechanical properties of the surface, making it less “sticky”. It can be seen that this stickiness decreases with an increase in erucamide concentration.

Author Contributions: Conceptualization, J.H.-F.; Methodology, J.L.-M.; Validation, J.H.-F., J.L.-M. and E.P.-P.; Formal analysis, J.H.-F.; Investigation, E.P.-P.; Writing—original draft preparation, J.L.-M.; Writing—review and editing, E.P.-P.; Supervision, J.H.-F.; Project administration, J.H.-F. All authors have read and agreed to the published version of the manuscript.

Funding: This research was supported by the Spanish Ministry of Science and Innovation/*Validación de los Materiales Sostenibles Obtenidos a Partir de Productos Naturales*/(PDC2021-121345-C22).

Institutional Review Board Statement: Not applicable.

Informed Consent Statement: Not applicable.

Data Availability Statement: Not applicable.

Conflicts of Interest: The authors declare no conflict of interest.

References

1. Chamas, A.; Moon, H.; Zheng, J.; Qiu, Y.; Tabassum, T.; Jang, J.H.; Abu-Omar, M.; Scott, S.L.; Suh, S. Degradation Rates of Plastics in the Environment. *ACS Sustain. Chem. Eng.* **2020**, *8*, 3494–3511. [CrossRef]
2. Hahladakis, J.N.; Velis, C.A.; Weber, R.; Iacovidou, E.; Purnell, P. An Overview of Chemical Additives Present in Plastics: Migration, Release, Fate and Environmental Impact during Their Use, Disposal and Recycling. *J. Hazard. Mater.* **2018**, *344*, 179–199. [CrossRef] [PubMed]
3. Bashir, I.; Lone, F.A.; Bhat, R.A.; Mir, S.A.; Dar, Z.A.; Dar, S.A. Concerns and Threats of Contamination on Aquatic Ecosystems. In *Bioremediation and Biotechnology*; Springer: Cham, Switzerland, 2020; pp. 1–26. [CrossRef]
4. Jaiswal, S.; Kumar Gupta, G.; Panchal, K.; Mandeep; Shukla, P. Synthetic Organic Compounds from Paper Industry Wastes: Integrated Biotechnological Interventions. *Front. Bioeng. Biotechnol.* **2021**, *8*, 592939. [CrossRef] [PubMed]
5. US EPA. Persistent Organic Pollutants: A Global Issue, A Global Response. Available online: <https://www.epa.gov/international-cooperation/persistent-organic-pollutants-global-issue-global-response> (accessed on 11 August 2022).
6. Grobelak, A.; Kowalska, A. Chapter 2—Emerging Environmental Contaminants—Current Status, Challenges, and Technological Solutions. In *Emerging Contaminants in the Environment*; Sarma, H., Dominguez, D.C., Lee, W.-Y., Eds.; Elsevier: Amsterdam, The Netherlands, 2022; pp. 39–53. ISBN 978-0-323-85160-2.
7. Hernández-Fernández, J.; Rodríguez, E. Determination of Phenolic Antioxidants Additives in Industrial Wastewater from Polypropylene Production Using Solid Phase Extraction with High-Performance Liquid Chromatography. *J. Chromatogr. A* **2019**, *1607*, 460442. [CrossRef]
8. Daughton, C.G. Non-Regulated Water Contaminants: Emerging Research. *Environ. Impact Assess. Rev.* **2004**, *24*, 711–732. [CrossRef]
9. Hurtado, C.; Domínguez, C.; Pérez-Babace, L.; Cañameras, N.; Comas, J.; Bayona, J.M. Estimate of Uptake and Translocation of Emerging Organic Contaminants from Irrigation Water Concentration in Lettuce Grown under Controlled Conditions. *J. Hazard. Mater.* **2016**, *305*, 139–148. [CrossRef]
10. Khetan, S.K.; Collins, T.J. Human Pharmaceuticals in the Aquatic Environment: A Challenge to Green Chemistry. *Chem. Rev.* **2007**, *107*, 2319–2364. [CrossRef]
11. Richardson, S.D.; Ternes, T.A. Water Analysis: Emerging Contaminants and Current Issues. *Anal. Chem.* **2018**, *90*, 398–428. [CrossRef]
12. Botalova, O.; Schwarzbauer, J.; Frauenrath, T.; Dsikowitzky, L. Identification and Chemical Characterization of Specific Organic Constituents of Petrochemical Effluents. *Water Res.* **2009**, *43*, 3797–3812. [CrossRef]

13. Förstner, U. Elements and Compounds in Waste Materials. In *Elements and Their Compounds in the Environment: Occurrence, Analysis and Biological Relevance*, 2nd ed.; Wiley Online Library: Hoboken, NJ, USA, 2004; pp. 163–197. ISBN 978-3-527-30459-2.
14. Ahmed, J.; Thakur, A.; Goyal, A. Chapter 1 Industrial Wastewater and Its Toxic Effects. In *Biological Treatment of Industrial Wastewater*; Royal Society of Chemistry: London, UK, 2021; pp. 1–14. [[CrossRef](#)]
15. Bart, J.C. Appendix II: Functionality of Common Additives Used in Commercial Thermoplastics, Rubbers and Thermosetting Resins. In *Additives in Polymers*; John Wiley & Sons, Ltd.: Hoboken, NJ, USA, 2005; pp. 773–791. ISBN 978-0-470-01206-2.
16. National Research Council. *Polymer Science and Engineering: The Shifting Research Frontiers*; National Academies Press: Washington, DC, USA, 1994.
17. De Paoli, M.A.; Aurelio, M.; Waldman, W. Bio-Based Additives for Thermoplastics. *Polímeros* **2019**, *29*, e2019030. [[CrossRef](#)]
18. Pfaendner, R. Polymer Additives. In *Handbook of Polymer Synthesis, Characterization, and Processing*; Saldívar-Guerra, E., Vivaldo-Lima, E., Eds.; John Wiley & Sons, Inc.: Hoboken, NJ, USA, 2013; pp. 225–247. ISBN 978-1-118-48079-3.
19. Gómez-Contreras, P.; Figueroa-Lopez, K.J.; Hernández-Fernández, J.; Cortés Rodríguez, M.; Ortega-Toro, R. Effect of Different Essential Oils on the Properties of Edible Coatings Based on Yam (*Dioscorea rotundata* L.) Starch and Its Application in Strawberry (*Fragaria vesca* L.) Preservation. *Appl. Sci.* **2021**, *11*, 11057. [[CrossRef](#)]
20. Pavon, C.; Aldas, M.; López-Martínez, J.; Hernández-Fernández, J.; Arrieta, M.P. Films Based on Thermoplastic Starch Blended with Pine Resin Derivatives for Food Packaging. *Foods* **2021**, *10*, 1171. [[CrossRef](#)]
21. Shao, J.; He, Y.; Li, F.; Zhang, H.; Chen, A.; Luo, S.; Gu, J.-D. Growth Inhibition and Possible Mechanism of Oleamide against the Toxin-Producing Cyanobacterium *Microcystis Aeruginosa* NIES-843. *Ecotoxicol. Lond. Engl.* **2016**, *25*, 225–233. [[CrossRef](#)]
22. Getachew, P.; Getachew, M.; Joo, J.; Choi, Y.S.; Hwang, D.S.; Hong, Y.K. The Slip Agents Oleamide and Erucamide Reduce Biofouling by Marine Benthic Organisms (Diatoms, Biofilms and Abalones). *Toxicol. Environ. Health Sci.* **2016**, *8*, 341–348. Available online: <https://link.springer.com/article/10.1007/s13530-016-0295-8> (accessed on 11 August 2022). [[CrossRef](#)]
23. Mitchell, C.A.; Davies, M.J.; Grounds, M.D.; McGeachie, J.K.; Crawford, G.J.; Hong, Y.; Chirila, T.V. Enhancement of Neovascularization in Regenerating Skeletal Muscle by the Sustained Release of Erucamide from a Polymer Matrix. *J. Biomater. Appl.* **1996**, *10*, 230–249. [[CrossRef](#)]
24. Wakamatsu, K.; Masaki, T.; Itoh, F.; Kondo, K.; Sudo, K. Isolation of Fatty Acid Amide as an Angiogenic Principle from Bovine Mesentery. *Biochem. Biophys. Res. Commun.* **1990**, *168*, 423–429. [[CrossRef](#)]
25. Hamberger, A.; Stenhagen, G. Erucamide Compounds for the Treatment and Prevention to Disturbances of the Secretory System. WIPO (PCT) WO2003002112A1, 9 January 2003.
26. Henzel, R.P.; Vanier, N.R. Slipping Layer Containing Functionalized Siloxane and Wax for Dye-Donor Element Used in Thermal Dye Transfer. U.S. Patent 4,866,026, 12 September 1989.
27. Catarino-Centeno, R.; Waldo-Mendoza, M.A.; Garcia-Hernandez, E.; Perez-Lopez, J.E. Relationship between the Coefficient of Friction of Additive in the Bulk and Chain Graft Surface Density through a Diffusion Process: Erucamide–Stearyl Erucamide Mixtures in Polypropylene Films. *J. Vinyl Addit. Technol.* **2021**, *27*, 459–466. Available online: <https://onlinelibrary.wiley.com/doi/10.1002/vnl.21820> (accessed on 11 August 2022). [[CrossRef](#)]
28. Kawamura, Y.; Miura, M.; Sugita, T.; Yamada, T.; Takeda, M. Simultaneous Determination of Antioxidants and Ultraviolet Stabilizers in Polyethylene by HPLC. *J. Food Hyg. Soc. Jpn.* **1996**, *37*, 272–279. [[CrossRef](#)]
29. Kawamura, Y.; Miura, M.; Sugita, T.; Yamada, T.; Takeda, M. Simultaneous Determination of Polymer Additives in Polyethylene by GC/MS. *J. Food Hyg. Soc. Jpn.* **1997**, *38*, 307–318. [[CrossRef](#)]
30. Kawamura, Y.; Yonezawa, R.; Maehara, T.; Yamada, T. Determination of additives in food contact polypropylene. *J. Food Hyg. Soc. Jpn.* **1997**, *41*, 154. [[CrossRef](#)]
31. Vandenburg, H.; Clifford, A.; Bartle, K.; Carroll, J.; Newton, I.; Garden, L.; Dean, J.; Costley, C. Critical Review: Analytical Extraction of Additives from Polymers. *Analyst* **1997**, *122*, 101–115. [[CrossRef](#)]
32. Roosen, M.; De Somer, T.; Demets, R.; Ugduler, S.; Meesseman, V.; Gorp, B.; Ragaert, K.; Van Geem, K.; Walgraeve, C.; Dumoulin, A.; et al. Towards a Better Understanding of Odor Removal from Post-Consumer Plastic Film Waste: A Kinetic Study on Deodorization Efficiencies with Different Washing Media. *Waste Manag.* **2020**, *120*, 564–575. [[CrossRef](#)] [[PubMed](#)]
33. Odor Removal—An Overview | ScienceDirect Topics. Available online: <https://www.sciencedirect.com/topics/engineering/odor-removal> (accessed on 11 August 2022).
34. Hernández-Fernández, J.; Lopez-Martínez, J.; Barceló, D. Quantification and Elimination of Substituted Synthetic Phenols and Volatile Organic Compounds in the Wastewater Treatment Plant during the Production of Industrial Scale Polypropylene. *Chemosphere* **2021**, *263*, 128027. [[CrossRef](#)] [[PubMed](#)]
35. Fernández, J.H.; Guerra, Y.; Cano, H. Detection of Bisphenol A and Four Analogues in Atmospheric Emissions in Petrochemical Complexes Producing Polypropylene in South America. *Molecules* **2022**, *27*, 4832. [[CrossRef](#)] [[PubMed](#)]
36. Hernández-Fernández, J.; Lopez-Martínez, J.; Barceló, D. Development and Validation of a Methodology for Quantifying Parts-per-Billion Levels of Arsine and Phosphine in Nitrogen, Hydrogen and Liquefied Petroleum Gas Using a Variable Pressure Sampler Coupled to Gas Chromatography-Mass Spectrometry. *J. Chromatogr. A* **2021**, *1637*, 461833. [[CrossRef](#)]
37. Hernández Fernández, J.; Cano, H.; Guerra, Y.; Puello Polo, E.; Ríos-Rojas, J.F.; Vivas-Reyes, R.; Oviedo, J. Identification and Quantification of Microplastics in Effluents of Wastewater Treatment Plant by Differential Scanning Calorimetry (DSC). *Sustainability* **2022**, *14*, 4920. [[CrossRef](#)]

38. Hernández-Fernández, J.; Guerra, Y.; Puello-Polo, E.; Marquez, E. Effects of Different Concentrations of Arsine on the Synthesis and Final Properties of Polypropylene. *Polymers* **2022**, *14*, 3123. [[CrossRef](#)]
39. Hernández-Fernández, J.; López-Martínez, J. Experimental Study of the Auto-Catalytic Effect of Triethylaluminum and TiCl₄ Residuals at the Onset of Non-Additive Polypropylene Degradation and Their Impact on Thermo-Oxidative Degradation and Pyrolysis. *J. Anal. Appl. Pyrolysis* **2021**, *155*, 105052. [[CrossRef](#)]
40. Hernández-Fernández, J.; Rayón, E.; López, J.; Arrieta, M.P. Enhancing the Thermal Stability of Polypropylene by Blending with Low Amounts of Natural Antioxidants. *Macromol. Mater. Eng.* **2019**, *304*, 1900379. [[CrossRef](#)]
41. Standard Test Method for Static and Kinetic Coefficients of Friction of Plastic Film and Sheeting. Available online: <https://www.astm.org/d1894-08.html> (accessed on 11 August 2022).
42. Joshi, N.B.; Hirt, D.E. Evaluating Bulk-to-Surface Partitioning of Erucamide in LLDPE Films Using FT-IR Microspectroscopy. *Appl. Spectrosc.* **1999**, *53*, 11–16. [[CrossRef](#)]
43. Huang, Y.; Xiong, Y.; Liu, C.; Li, L.; Xu, D.; Lin, Y.-H.; Nan, C.-W. Single-Crystalline 2D Erucamide with Low Friction and Enhanced Thermal Conductivity. *Colloids Surf. Physicochem. Eng. Asp.* **2018**, *540*, 29–35. [[CrossRef](#)]
44. Har-Even, E.; Brown, A.; Meletis, E.I. Effect of Friction on the Microstructure of Compacted Solid Additive Blends for Polymers. *Wear* **2015**, *328–329*, 160–166. [[CrossRef](#)]
45. Soliman, M.; Essers, F.E.J.; Degenhart, P. Scratch-Resistant Moulded Article Made from a Filled Polypropylene Composition. U.S. Patent US8163378B2, 19 November 2009.

Disclaimer/Publisher’s Note: The statements, opinions and data contained in all publications are solely those of the individual author(s) and contributor(s) and not of MDPI and/or the editor(s). MDPI and/or the editor(s) disclaim responsibility for any injury to people or property resulting from any ideas, methods, instructions or products referred to in the content.